



Published in final edited form as:

Otol Neurotol. 2022 December 01; 43(10): 1155–1161. doi:10.1097/MAO.0000000000003707.

Comparative Analysis of Robotics-Assisted and Manual Insertions of Cochlear Implant Electrode Arrays

Alexander D. Claussen*, Seiji B. Shibata*, Christopher R. Kaufmann†, Allan Henslee†, Marlan R. Hansen*,†

*Department of Otolaryngology–Head and Neck Surgery, University of Iowa

†iotaMotion, Inc., Iowa City, Iowa

Abstract

Hypothesis: Robotics-assisted cochlear implant (CI) insertions will result in reduced intracochlear trauma when compared with manual, across multiple users.

Background: Whether intracochlear trauma and translocations are two factors that may contribute to significant variability in CI outcomes remains to be seen. To address this issue, we have developed a robotics-assisted insertion system designed to aid the surgeon in inserting electrode arrays with consistent speeds and reduced variability. This study evaluated the effect of robotics-assisted insertions on the intracochlear trauma as compared with manual insertions in cadaveric cochleae in a simulated operative environment.

Methods: Twelve neurotologists performed bilateral electrode insertions into cochleae of full cadaveric heads using both the robotics-assisted system and manual hand insertion. Lateral wall electrodes from three different manufacturers ($n = 24$) were used and randomized between surgeons. Insertion angle of the electrode and trauma scoring were evaluated using high-resolution three-dimensional x-ray microscopy and compared between robotics-assisted and manual insertions.

Results: Three-dimensional x-ray microscopy provided excellent resolution to characterize the in situ trauma and insertion angle. Robotics-assisted insertions significantly decreased insertional intracochlear trauma as measured by reduced trauma scores compared with manual insertions (average: 1.3 versus 2.2, device versus manual, respectively; $p < 0.05$). There was no significant difference between insertion angles observed for manual and robotics-assisted techniques ($311 \pm 131^\circ$ versus $307 \pm 96^\circ$, device versus manual, respectively).

Conclusions: Robotics-assisted insertion systems enable standardized electrode insertions across individual surgeons and experience levels. Clinical trials are necessary to investigate whether insertion techniques that reduce insertional variability and the likelihood of intracochlear trauma also improve CI auditory outcomes.

Address correspondence and reprint requests to Alexander D. Claussen, M.D., Division of Head and Neck Surgery, University of California—San Diego, 200 W. Arbor Drive, San Diego, CA 92103; aclaussen@ucsd.edu.
Current affiliation of A.D.C.: Department of Otolaryngology, University of California—San Diego, San Diego, California.
Current affiliation of S.B.S.: Department of Otolaryngology–Head and Neck Surgery, University of Southern California, Los Angeles, California.

Keywords

Cochlear implantation; Cochlear trauma; Hearing preservation; Hybrid; Robotics; Robotics-assisted

INTRODUCTION

Preservation of the structure and function in the cochlea during insertion of a cochlear implant (CI) has become a high priority for improving patient outcomes. For example, disruptive intracochlear trauma due to electrode array insertion, such as scalar translocation, is associated with diminished performance (1). Furthermore, the paradigm of hearing preservation cochlear implantation has greatly expanded the traditional CI candidate population to include those with primarily high-frequency hearing loss and preserved low-frequency hearing (2). The performance benefits of electroacoustic stimulation associated with hearing preservation cochlear implantation, including improved music and speech perception and sound localization relative to traditional CI, are contingent on maintaining serviceable, residual low-frequency hearing after implantation (3). Although several studies from high-volume CI centers have shown high rates of maintaining serviceable hearing after implantation, there is still significant variability in auditory outcomes based on surgeon/center experiences, patient factors, etiology of hearing loss, and electrode type (4–8). Furthermore, approximately 50% of patients will still experience delayed loss of the preoperative hearing levels (>10 dB change in pure-tone average) after surgery (4–8).

The pathophysiologic events resulting in loss of residual acoustic hearing after cochlear implantation are diverse and may involve neural and/or sensory cell degeneration as well as an intracochlear conductive hearing loss resulting from CI-associated fibrosis and neossification (9–13). Ample evidence suggests that the intracochlear surgical trauma from implantation negatively affects traditional CI outcomes as well as contributing to loss of residual acoustic hearing (1,14–16). Following from these observations, multiple strategies have been developed to reduce implantation trauma in an effort to improve outcomes and hearing preservation, including physical electrode design, pharmacologic adjuncts, electrode coatings (e.g., antifouling or lubricating), electrophysiologic monitoring, and emphasis on “soft” surgical technique (reviewed by Tarabichi et al. (17)). Of these factors, the surgical electrode insertion and the ability to make real-time insertion adjustments in response to electrophysiologic feedback are most limited by human factors, suggesting the potential utility of a robotics-assisted electrode insertion tool.

One of the main limitations in soft surgical placement of a CI is the kinematic constraints of human movement, which have shown to limit the slowest human continuous implantation speed to 867 $\mu\text{m/s}$ (18). Insertion speeds are found to positively correlate with insertion forces, and high insertion forces have been associated with increased intracochlear structural trauma and intracochlear pressure spikes, which can cause damage to the inner ear similar to loud noise exposure and damage residual hearing (19–24). Following from this, use of robotics-assisted insertion tools in cadaveric studies has demonstrated the ability to achieve

slower continuous insertion speeds with lower insertion forces and peak pressure spikes than that achievable with human operators (25).

We have previously published preliminary results of a robotics-assisted CI insertion tool, which achieved slower CI insertion speeds and forces with a reduced rate of intracochlear traumatic events compared with manual CI insertion in cadaveric human temporal bones (26). Here we expand on previous work comparing CI insertion metrics, including insertion angle and three-dimensional (3-D) x-ray microscopic intracochlear trauma grading (modified by Eshraghi et al. (27)), between manual and robotics-assisted CI insertions performed on fresh-frozen full human cadaveric heads by experienced neurotologists. Development, validation, and adoption of a robotics-assisted CI insertion tool capable of performing atraumatic CI insertions with improved structural and functional cochlear preservation may ultimately benefit patients by both improving CI performance and increasing the consistency of CI outcomes across surgeons/ centers, thus expanding the access to this form of auditory rehabilitation.

MATERIALS AND METHODS

Manual Versus Robotics-Assisted CI Insertion in Full Frozen Human Cadaveric Heads

This study compared manual ($n = 12$) versus robotics-assisted ($n = 12$) CI insertion by attending neurotologists ($n = 12$) in fresh-frozen full human cadaveric heads, with each surgeon performing both methods of insertion on randomized, opposing sides of a single head. Fresh-frozen human heads ($n = 12$ heads; $n = 24$ cochleae) were thawed as previously described (26). A separate team surgeon (attending neurotologist or second-year neurology fellow with review by attending neurotologist) prepared each head for CI insertion by following the usual steps for mastoidectomy with facial recess, including use of standard operative equipment, draping, and incisions, similar to that used in typical CI surgery. Before opening the oval and round window, the operative field was thoroughly irrigated to remove bone dust. The oval and round windows were opened with a needle, and a 10% soap/phosphate-buffered saline solution was slowly infused through the oval window until fluid egress from the round window was observed; this served to lubricate the cadaver tissues before CI insertion.

Before the insertion procedure, the user surgeons underwent device training for the robotics-assisted system (iotaSOFT Insertion System; iotaMotion Inc., Iowa City, IA) and were given additional time to review instructions for use material. The robotics-assisted system and insertion process is overviewed in Figure 1. A 1-hour time period elapsed between training and robotics-assisted CI insertion to account for any training decay. This robotics-assisted system is designed to be compatible across multiple CI electrode array designs, and users were randomly assigned to insert one of three different lateral wall electrodes (Advanced Bionics Slim J (Advanced Bionics Corporation, Valencia, California), Cochlear Slim Straight (Cochlear Limited, Sydney, Australia), MedEl Flex24 (MedEL, Innsbruck, Austria)) for both manual and robotics-assisted CI insertions. Users began with robotics-assisted CI insertion on a randomly assigned ear side and then proceeded with manual insertion on the contralateral ear using standard surgical instruments.

Specimen Preparation

Immediately after insertion on each side, the electrode array was secured in place with Loctite 401 (Henkel Adhesive Technologies, Rocky Hill, CT) application just outside the cochlea. Next, tissue fixation was performed by gently perfusing 20 ml of 4% paraformaldehyde solution through the oval window using a syringe, with care made to avoid disrupting the electrode position. After bilateral cochlear implantation, electrode securement, and tissue fixation, the bilateral temporal bones were harvested following the technique described by Nadol et al. (28). Temporal bones were stored in 4% paraformaldehyde for 7 days and then underwent serial dehydration in ethanol solution (70–100%). Next, excess fluid was suctioned from the cochlea at the oval and round windows and the specimen further desiccated in a vacuum chamber. As a final step, excessive bone was removed with rongeurs to isolate the otic capsule to facilitate 3-D x-ray microscopy.

3-D X-ray Microscopy and Image Analysis

This group has previously described the use of 3-D x-ray microscopy for nondestructive qualitative and semiquantitative analyses of CI insertional trauma (26). This technique allows high-resolution (voxel size, $6 \times 6 \times 6$ to $12 \times 12 \times 12 \mu\text{m}^3$) imaging of soft and hard (bone) tissue structures of the cochlea with the in situ electrode overlaid, allowing assessment of insertion depth, intracochlear trauma, and scalar positioning relative to native cochlear structures (i.e., basilar membrane, Reisner's membrane, spiral ligament and osseus spiral lamina [OSL]).

Processed samples were imaged with a Zeiss Xradia 520 Versa high-resolution 3-D x-ray microscopy system (Zeiss, Jena, Germany). Image spatial resolution ranged from 6 to 12 μm per scan, depending on the field of view. Temporal bone specimens were first imaged with the electrode array left in situ and then again in the exact same spatial positioning with the electrode array removed. The two image sets were overlaid into a composite image set and co-registered using reliable bony landmarks for exact image alignment; the “electrode in situ” image series was then windowed to heavily weight the electrode array, and the “electrode removed” image series was windowed to highlight both soft and hard tissue, with the resulting composite image displaying the cochlea with electrode array in situ minus any electrode associated artifact. The composite image production and analysis was performed using Dragonfly visual software suite (ORS, Montréal Canada).

Image analysis was performed by an examiner familiar with radiologic and histologic intracochlear anatomy and blinded to experimental condition. Trauma scoring was performed according to a previously published 3-D x-ray microscopy trauma grading scale based on estimates of clinical severity of different trauma events (26). Intracochlear trauma events identified on composite image sets were confirmed on the reference electrode in situ image stacks to ensure that there was no artifact from electrode array removal that may alter trauma grading. Electrode insertion angle was determined following a strategy similar to that previously described in histologic and radiologic images (29). 3-D image reconstructions were oriented to a plane perpendicular to the long axis of the modiolus, with the image projection depth sufficiently heightened so that all implant electrodes and the round window were visible. Insertion angle was calculated from the intersection of two lines originating at

the modiolus and drawn through the center of the round window and the other through the most apical electrode tip. Statistical comparisons of trauma grading between the manual and robotics-assisted groups were performed via a Wilcoxon rank test with significance defined at $p < 0.05$ using JMP statistical software (SAS Institute, Cary, NC).

RESULTS

Manual Versus Robotics-Assisted Insertion

Study characteristics and results are shown in Table 1, and individual surgeon outcomes are shown in Table 2. Attending surgeons had a mean of 21.7 years of practice (median, 22 yr), performed a mean of 103 cochlear implantations in the past year (ranging from 10 to 500; standard deviation, 130) and were all right-hand dominant. A balanced distribution of CI electrode array models was allocated to both the manual and robotics-assisted insertion groups, with the MedEL Flex 24 being the most common array inserted. The manual insertion group was assigned more left ($n = 7$) than right ($n = 5$) ears and the opposite finding occurring in the robotics-assisted group. Similar mean insertion angles were achieved in the manual (mean, $311 \pm 131^\circ$) and robotics-assisted (mean, $307 \pm 96^\circ$). Notably, the electrode was accidentally partially removed from Surgeon 10's manual insertion specimen during sample preparation, before insertion angle measurement, artifactually influencing the short 41° insertion angle observed. Tip fold-over was observed more often in the manual ($n = 2$) compared with robotics-assisted ($n = 1$) group. Overall, user surgeons were able to successfully achieve a round window insertion of the CI in both the manual and robotics-assisted groups without any extracochlear insertions.

Intracochlear Insertion Trauma Assessment

Quantitative trauma assessment was graded according to the scale shown in Table 3. Demonstrative images of the 2-D and 3-D composite image reconstructions used for quantitative and qualitative analyses are shown in Figure 2 (see Supplemental Digital Content 1, <http://links.lww.com/MAO/B501>, which demonstrates 2-D and 3-D reconstructions for the additional 22 samples not included in Fig. 2). Overall, the robotics-assisted group had a significantly lower mean trauma grade of 1.33 ± 0.98 compared with the manual insertion group mean trauma grade of 2.17 ± 1.34 ($p < 0.05$; mean difference, -0.833 ; 95% confidence interval, -1.59 to -0.075). Figure 3 plots the distribution of trauma grades between the groups. Scala media translocation (grade 2) was the most common event in both groups and no grade 5 events (OSL fracture and scalar translocation) were seen in either group. The highest-grade event occurring in the robotics-assisted group was grade 3 ($n = 1$) compared with grade 4 ($n = 3$) in the manual insertion group. The robotics-assisted group had more ($n = 3$) atraumatic, grade 0 insertions than the manual group ($n = 1$). Trauma grade was lower with the robotics-assisted compared with manual insertion for seven surgeons, the same for three surgeons and higher for two surgeons.

Scala media translocation (grade 2) occurred more often in the distal (apical) half of the CI insertion depth, whereas basilar membrane elevation (grade 1) was seen to occur at any point along the CI insertion depth. Tip fold-over was exclusively associated with grade 1 ($n = 1$) and grade 2 ($n = 2$) trauma and not seen at higher trauma grades. Surgeon 4

(100 CI procedures per year) experienced tip fold-over in both manual and robotics-assisted insertions, and surgeon 2 (10 CI procedures per year) experienced the tip fold-over with manual insertion only. No specific observations were made by the implanting surgeons or experimenters at the time of CI insertion to predict tip fold-over. OSL fracture (grade 4) events were confined to the round window area and basal turn.

DISCUSSION

Robotics-assisted CI insertion was associated with significantly less intracochlear trauma when compared with standard manual insertion by experienced neurotologic surgeons who were newly trained on the robotics-assisted system use. The maximum and overall mean insertion trauma grades observed with robotics-assisted CI insertion were significantly less than manual insertion. In addition, the number of grade 0, atraumatic insertions was higher with robotics-assisted CI insertion. The results of this study are consistent with previous work examining robotics-assisted versus manual CI insertion performed by surgeons of varying degrees of experience (resident, fellow, and attending levels), where less insertion trauma was seen in the robotics-assisted group, and grade 4 and higher trauma scores were exclusively associated with manual CI insertion (26).

Previous work using a similar robotics-assisted CI insertion tool has demonstrated the ability to achieve lower maximum force and force variation during CI insertion as compared with manual insertion (25,26). In addition, other studies have shown that the CI insertional force has been positively correlated with intracochlear trauma events (30). After this evidence, we hypothesize the slower and lower force CI insertion from the robotics-assisted CI insertion tool results in less intracochlear trauma when compared with the more variable speed and higher force manual insertions.

In the past two decades, multiple groups have developed devices aimed at facilitating electrode insertion or cochlear exposure, reviewed most recently by De Seta et al. (31) and Panara et al. (32). Multiple design strategies have been implemented across electrode insertion devices, with the goal of achieving less traumatic CI insertions through controlling insertion force, speed, and vector (21,25,33–36). Previous preclinical studies have demonstrated success across multiple insertion devices in reducing scalar translocation or intracochlear trauma over manual insertion (26,37). The current study examines an additional factor inherent to the successful clinical implementation of CI insertion devices: consistency and ease of use by multiple different surgeons. Future and ongoing clinical trials are necessary to examine the clinical utility of these devices in improving CI auditory outcomes.

The spectrum of CI insertional traumatic events has been well studied in both fresh-frozen cadaveric models of CI implantation and postmortem CI recipients (27,38–40). Previous trauma grading scales have been created based on estimates of the physiologic consequence of histologically identified traumatic events, including scalar translocations, OSL fracture, and lateral wall damage (27,30,38). The current study used a recently published radiologic trauma grading scale specific to high-resolution 3-D x-ray microscopy (26). These strategies are limited by several aspects, including the limited ability to clinically validate the

the surgeon subjects having already been prepared with mastoidectomy and facial recess, which may disorient the implanting surgeon to the surgical anatomy, having not performed the usual previous surgical steps themselves. Although the cochlear soft tissue and bony architecture is preserved in fresh cadaveric heads, it is possible that the absence of blood flow and other homeostatic mechanisms may change intracochlear fluid (e.g., lubricity) and tissue dynamics (e.g., tensile strength of the basilar membrane) and alter the resulting CI insertional trauma. In addition, by nature of this being a cadaveric model, we are unable to make observations on the subsequent pathophysiologic sequela of the observed insertional trauma (e.g., intracochlear fibrosis) or on actual hearing and CI performance outcomes. However, fresh cadaveric heads may be better suited than other alternative nonanimal preclinical models, including 3-D printed temporal bones, which lack soft tissue elements for which insertion trauma affects, and fixed cadaveric temporal bones, in which the fixation process may artificially stiffen intracochlear soft tissue elements and impart extra resilience to CI insertion trauma.

Taken together with previous studies, this study demonstrates the ability of a robotics-assisted CI insertional systems to achieve more consistent and less traumatic CI insertions in a surgical simulation model than the current manual insertion practices. Further clinical trials may be needed to confirm the effectiveness of robotics-assisted CI insertion to reduce cochlear trauma and potentially improve clinical CI outcomes and hearing preservation rates.

CONCLUSION

CI performance has benefited by advances in electrode design and programming strategies but is still subject to human kinematic limitations during surgical insertion. A robotics-assisted insertion device represents one strategy to potentially overcome these human factor limitations and improve CI outcomes. The standardization and stabilization inherent to a robotics-assisted insertion relative to the current manual CI insertion practices may allow the broader access to consistent, less traumatic CI insertions that are necessary to meet the needs of the increasing global CI candidate population.

Supplementary Material

Refer to Web version on PubMed Central for supplementary material.

Acknowledgments:

The authors thank Michael Acevedo and Susan Walsh at the Small Animal Imaging Core, University of Iowa College of Medicine, Department of Radiology and Nuclear Medicine, for technical assistance on Xradia system (National Institutes of Health 1S10OD018503-01); the University of Miami CANES Lab for surgical simulation laboratory support; and Cochlear, Advanced Bionics, and MedEl for supplying test electrodes.

Sources of support and disclosure of funding:

C.R.K. and M.R.H. are co-founders and directors of iotaMotion, Inc. A.H. is an iotaMotion employee. For the remaining authors, there are no conflicts of interest to report. Funding was provided by iotaMotion, Inc., and the National Institute on Deafness and Other Communication Disorders (T32 DC00040).

REFERENCES

1. Carlson ML, Driscoll CLW, Gifford RH, et al. Implications of minimizing trauma during conventional cochlear implantation. *Otol Neurotol* 2011;32:962–8. [PubMed: 21659922]
2. Goman AM, Dunn CC, Gantz BJ, Lin FR. Prevalence of potential hybrid and conventional cochlear implant candidates based on audiometric profile. *Otol Neurotol* 2018;39:515–7. [PubMed: 29498962]
3. Gantz BJ, Dunn CC, Oleson J, Hansen MR. Acoustic plus electric speech processing: Long-term results. *Laryngoscope* 2018;128:473–81. [PubMed: 28543270]
4. Gantz BJ, Hansen MR, Turner CW, et al. Hybrid 10 clinical trial: Preliminary results. *Audiol Neurotol*. 2009;14(Suppl 1):32–8.
5. Roland JT, Gantz BJ, Waltzman SB, Parkinson AJ. United States multicenter clinical trial of the cochlear nucleus hybrid implant system. *Laryngoscope* 2016;126:175–81. [PubMed: 26152811]
6. Lenarz T, James C, Cuda D, et al. European multi-centre study of the Nucleus Hybrid L24 cochlear implant. *Int J Audiol* 2013;52:838–48. [PubMed: 23992489]
7. Gantz BJ, Dunn C, Oleson J, et al. Multicenter clinical trial of the nucleus hybrid S8 cochlear implant: Final outcomes. *Laryngoscope* 2016;126:962–73. [PubMed: 26756395]
8. Scheperle RA, Tejani VD, Omtvedt JK, et al. Delayed changes in auditory status in cochlear implant users with preserved acoustic hearing. *Hear Res* 2017;350:45–57. [PubMed: 28432874]
9. Tejani VD, Kim JS, Oleson JJ, et al. Residual hair cell responses in electric-acoustic stimulation cochlear implant users with complete loss of acoustic hearing after implantation. *J Assoc Res Otolaryngol* 2021;22:161–76. [PubMed: 33538936]
10. Kopelovich JC, Reiss LAJ, Etlar CP, et al. Hearing loss after activation of hearing preservation cochlear implants might be related to afferent cochlear innervation injury. *Otol Neurotol* 2015;36:1035–44. [PubMed: 25955750]
11. Quesnel AM, Nakajima HH, Rosowski JJ, et al. Delayed loss of hearing after hearing preservation cochlear implantation: Human temporal bone pathology and implications for etiology. *Hear Res* 2016;333:225–34. [PubMed: 26341474]
12. Claussen AD, Quevedo RV, Mostaert B, et al. A mouse model of cochlear implantation with chronic electric stimulation. *PLoS One* 2019;14:e0215407.
13. Heutink F, Klabbbers TM, Huinck WJ, et al. Ultra-high-resolution CT to detect intracochlear new bone formation after cochlear implantation. *Radiology* 2021;302:605–12. [PubMed: 34874202]
14. Eshraghi AA, Polak M, He J, et al. Pattern of hearing loss in a rat model of cochlear implantation trauma. *Otol Neurotol* 2005;26:442–7. [PubMed: 15891647]
15. Kopelovich JC, Robinson BK, Soken H, et al. Acoustic hearing after murine cochlear implantation: Effects of trauma and implant type. *Ann Otol Rhinol Laryngol* 2015;124:931–9. [PubMed: 26091845]
16. Knoll RM, Trakimas DR, Wu MJ, et al. Intracochlear new fibroossification and neuronal degeneration following cochlear implant electrode translocation: Long-term histopathological findings in humans. *Otol Neurotol* 2022;43:e153–64. [PubMed: 35015749]
17. Tarabichi O, Jensen M, Hansen MR. Advances in hearing preservation in cochlear implant surgery. *Curr Opin Otolaryngol Head Neck Surg* 2021;29:385–90. [PubMed: 34354014]
18. Kesler K, Dillon NP, Fichera L, Labadie RF. Human kinematics of cochlear implant surgery: An investigation of insertion micro-motions and speed limitations. *Otolaryngol Head Neck Surg* 2017;157:493–8. [PubMed: 28508720]
19. Kontorinis G, Lenarz T, Stöver T, Paasche G. Impact of the insertion speed of cochlear implant electrodes on the insertion forces. *Otol Neurotol* 2011;32:565–70. [PubMed: 21478788]
20. Rajan GP, Kontorinis G, Kuthubutheen J. The effects of insertion speed on inner ear function during cochlear implantation: A comparison study. *Audiol Neurootol* 2012;18:17–22. [PubMed: 23006502]
21. Majdani O, Schurzig D, Hussong A, et al. Force measurement of insertion of cochlear implant electrode arrays in vitro: Comparison of surgeon to automated insertion tool. *Acta Otolaryngol* 2010;130:31–6. [PubMed: 19484593]

22. Mirsalehi M, Rau TS, Harbach L, et al. Insertion forces and intracochlear trauma in temporal bone specimens implanted with a straight atraumatic electrode array. *Eur Arch Otorhinolaryngol* 2017;274:2131–40. [PubMed: 28238160]
23. Todt I, Mittmann P, Ernst A. Intracochlear fluid pressure changes related to the insertional speed of a CI electrode. *Biomed Res Int* 2014;2014:1–4.
24. Greene NT, Mattingly JK, Banakis Hartl RM, Tollin DJ, Cass SP. Intracochlear pressure transients during cochlear implant electrode insertion. *Otol Neurotol* 2016;37:1541–8. [PubMed: 27753703]
25. Banakis Hartl RM, Kaufmann C, Hansen MR, Tollin DJ. Intracochlear pressure transients during cochlear implant electrode insertion: Effect of micro-mechanical control on limiting pressure trauma. *Otol Neurotol* 2019;40:736–44. [PubMed: 31192901]
26. Kaufmann CR, Henslee AM, Claussen A, Hansen MR. Evaluation of insertion forces and cochlear trauma following robotics-assisted cochlear implant electrode array insertion. *Otol Neurotol* 2020;41:631–8. [PubMed: 32604327]
27. Eshraghi AA, Yang NW, Balkany TJ. Comparative study of cochlear damage with three perimodiolar electrode designs. *Laryngoscope* 2003; 113:415–9. [PubMed: 12616189]
28. Nadol J, Adams J, Cody DT, et al. Techniques for human temporal bone removal: Information for the scientific community. *Otolaryngol Head Neck Surg* 1996;115:298–305. [PubMed: 8861882]
29. Verbist BM, Skinner MW, Cohen LT, et al. Consensus panel on a cochlear coordinate system applicable in histologic, physiologic, and radiologic studies of the human cochlea. *Otol Neurotol* 2010; 31:722–30. [PubMed: 20147866]
30. Adunka O, Kiefer J. Impact of electrode insertion depth on intracochlear trauma. *Otolaryngol Head Neck Surg* 2006;135:374–82. [PubMed: 16949967]
31. De Seta D, Daoudi H, Torres R, et al. Robotics, automation, active electrode arrays, and new devices for cochlear implantation: A contemporary review. *Hear Res* 2022;414:108425.
32. Panara K, Shahal D, Mittal R, Eshraghi AA. Robotics for cochlear implantation surgery: Challenges and opportunities. *Otol Neurotol* 2021;42:e825–35. [PubMed: 33993143]
33. Hussong A, Rau TS, Ortmaier T, et al. An automated insertion tool for cochlear implants: Another step towards atraumatic cochlear implant surgery. *Int J Comput Assist Radiol Surg* 2010;5:163–71. [PubMed: 20033518]
34. Schurzig D, Webster RJ, Dietrich MS, Labadie RF. Force of cochlear implant electrode insertion performed by a robotic insertion tool: Comparison of traditional versus advance off-stylet techniques. *Otol Neurotol* 2010;31:1207–10. [PubMed: 20814345]
35. Rau TS, Zuniga MG, Salcher R, Lenarz T. A simple tool to automate the insertion process in cochlear implant surgery. *Int J Comput Assist Radiol Surg* 2020;15:1931–9. [PubMed: 32857248]
36. Torres R, Drouillard M, De Seta D, et al. Cochlear implant insertion axis into the basal turn: A critical factor in electrode array translocation. *Otol Neurotol* 2018;39:168–76. [PubMed: 29194215]
37. Torres R, Jia H, Ne Drouillard M, et al. An optimized robot-based technique for cochlear implantation to reduce array insertion trauma. *Otolaryngol Head Neck Surg* 2018;159:900–7. [PubMed: 30084309]
38. Roland PS, Wright CG. Surgical aspects of cochlear implantation: Mechanisms of insertional trauma. *Adv Otorhinolaryngol* 2006;64: 11–30. [PubMed: 16891834]
39. Ishai R, Herrmann BS, Nadol JB, Quesnel AM. The pattern and degree of capsular fibrous sheaths surrounding cochlear electrode arrays. *Hear Res* 2017;348:44–53. [PubMed: 28216124]
40. Li P, Somdas MA, Eddington DK, Nadol JB. Analysis of intracochlear new bone and fibrous tissue formation in human subjects with cochlear implants. *Ann Otol Rhinol Laryngol* 2007;116:731–8. [PubMed: 17987778]
41. Kamakura T, Nadol JB. Correlation between word recognition score and intracochlear new bone and fibrous tissue after cochlear implantation in the human. *Hear Res* 2016;339:132–41. [PubMed: 27371868]
42. Zuniga MG, Rivas A, Hedley-Williams A, et al. Tip fold-over in cochlear implantation: Case series. *Otol Neurotol* 2017;38:199–206. [PubMed: 27918363]
43. Dhanasingh A, Jolly C. Review on cochlear implant electrode array tip fold-over and scalar deviation. *J Otol* 2019;14:94–100. [PubMed: 31467506]

44. Frisch CD, Carlson ML, Lane JI, Driscoll CLW. Evaluation of a new mid-scala cochlear implant electrode using microcomputed tomography. *Laryngoscope* 2015;125:2778–83. [PubMed: 25946683]
45. Trakimas DR, Kozin ED, Ghanad I, et al. Precurved cochlear implants and tip foldover: A cadaveric imaging study. *Otolaryngol Head Neck Surg* 2018;158:343–9. [PubMed: 29086634]
46. Carlson ML, Leng S, Diehn FE, et al. Cochlear implant electrode localization using an ultra-high resolution scan mode on conventional 64-slice and new generation 192-slice multi-detector computed tomography. *Otol Neurotol* 2017;38:978–84. [PubMed: 28570418]

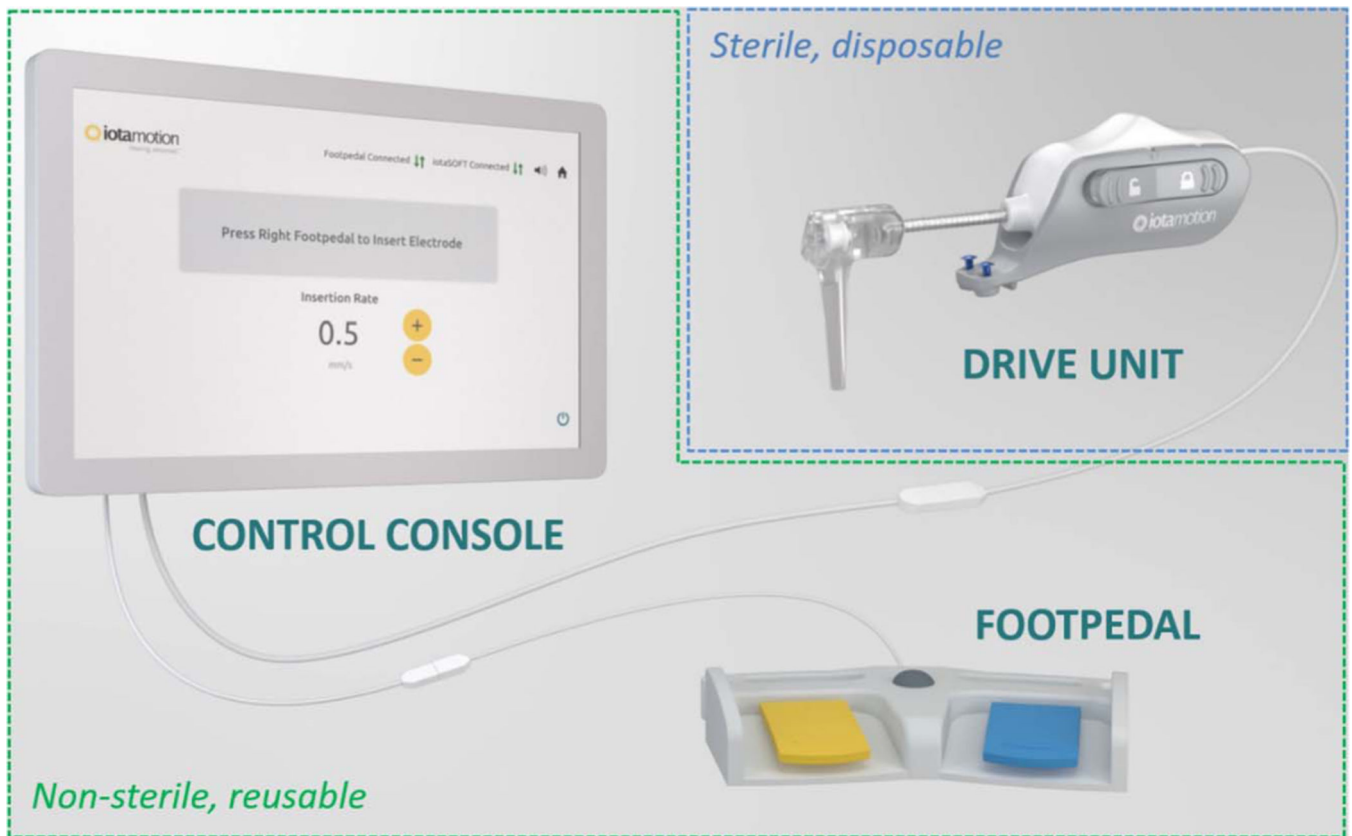
**FIG. 1.**

Diagram of robotics-assisted CI insertion system. The robotic system comprises two basic components—a sterile, disposable drive unit, which interfaces with the electrode array (outlined in blue), and a reusable control console/footpedal (outlined in green), which allows the user to control the speed of insertion in a “hands-free” manner. In brief, the robotics-assisted cochlear implantation was accomplished in three basic steps after the mastoidectomy. First, the drive unit was aligned with the facial recess and attached to the skull using the self-tapping screws. Next, the surgeon loaded the drive unit with the assigned electrode array and achieved the desired trajectory through manipulation of a movable head. Then, using the control console and footpedal, the electrode array was inserted into the cochlea at a desired speed. Lastly, the drive unit was detached from the electrode array and the skull, and the surgeon glued the electrode in place before explanation of the cochlea. CI indicates cochlear implant.

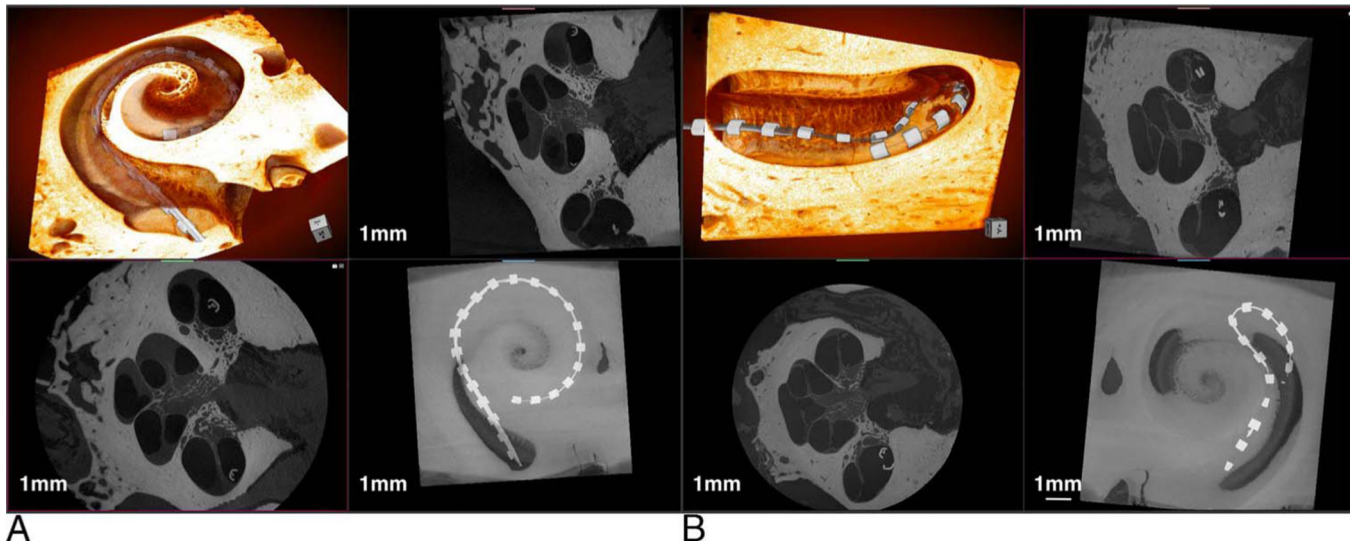


FIG. 2. Demonstrative images of 3-D x-ray microscopy. Image (A) demonstrate a scala tympani robotics-assisted insertion with associated 3-D and 2-D composite reconstructions. B, shows a manual scala tympani CI insertion with tip fold-over on similar composite reconstructions. CI indicates cochlear implant; 2-D/3-D, two/three-dimensional.

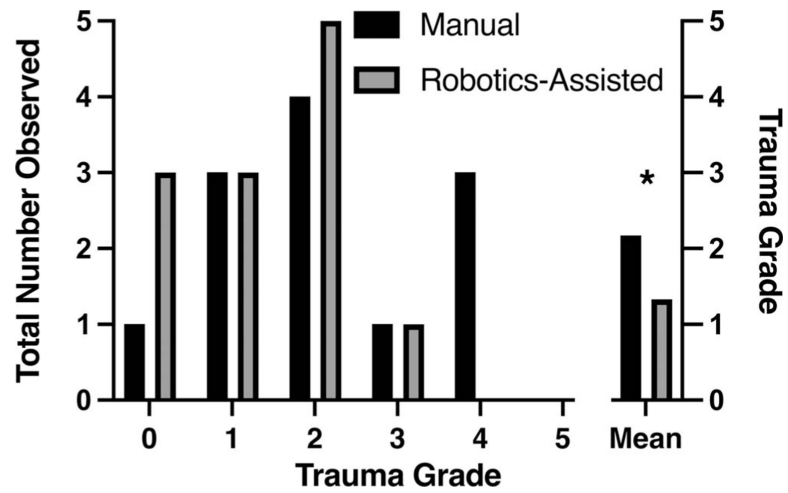


FIG. 3.

Trauma scoring. The distribution of scored trauma grades between groups is plotted as the absolute number of grades assigned. The mean group trauma score is plotted on the right-hand side. The manual insertion group had a significantly greater mean trauma grade compared with the robotics-assisted group. “*” denotes significant differences ($p < 0.05$).

TABLE 1.

Baseline study characteristics

	Manual	Robotics-Assisted
CI model		
Advanced Bionics		
SlimJ	2	2
MedEL Flex 24	6	6
Cochlear Slim Straight	4	4
Ear laterality		
Left	7	5
Right	5	7
Mean insertion angle (°)	311 ± 131	307 ± 96
Tip fold-over events	2	1

CI indicates cochlear implant.

Author Manuscript

Author Manuscript

Author Manuscript

Author Manuscript

TABLE 2.

Individual surgeon outcomes

Surgeon	Implantations in Last year ^a	Laterality	Insertion Method	Implant Model	Trauma Grade	Insertion Angle (°)
1	75	L	Manual	AB	2	328
		R	RA		0	258
2	10	L	Manual	MED-EL	1	474 ^b
		R	RA		1	133
3	50	L	Manual	MED-EL	1	195
		R	RA		0	357
4	100	L	Manual	Cochlear	2	303 ^b
		R	RA		1	163 ^b
5	125	L	Manual	MED-EL	3	443
		R	RA		3	266
6	80	L	RA	MED-EL	1	358
		R	Manual		0	136
7	60	L	RA	AB	2	232
		R	Manual		4	285
8	120	L	Manual	MED-EL	1	398
		R	RA		2	448
9	500	L	RA	Cochlear	0	372
		R	Manual		2	309
10	35	L	RA	MED-EL	2	378
		R	Manual		4	41 ^c
11	25	L	RA	Cochlear	2	370
		R	Manual		4	400
12	55	L	Manual	Cochlear	2	416
		R	RA		2	355

^aResponse to question: approximately how many cochlear implantations have you performed in the last year?

^bDenotes tip fold over.

^cCochlear implant was partially removed during specimen preparation, before insertion angle measurement.

L indicates left; R, right; RA, robotics-assisted.

Author Manuscript

Author Manuscript

Author Manuscript

Author Manuscript

TABLE 3.

X-ray microscopy insertion trauma scoring

Grade^a	Trauma Event
0	No macroscopic trauma
1	Basilar membrane elevation
2	Scala media translocation
3	Scala vestibuli translocation
4	OSL fracture
5	OSL fracture + translocation

^aGrade assigned based on the highest trauma event identified.

OSL indicates osseus spiral lamina.

Inspired by Kaufmann et al. (26).

Author Manuscript

Author Manuscript

Author Manuscript

Author Manuscript